



**HAL**  
open science

# Synthesis and study of $\gamma$ -Fe<sub>2</sub>O<sub>3</sub> and CoFe<sub>2</sub>O<sub>4</sub> based ferrofluids by means of spectroscopic Mueller matrix ellipsometry

Yann Battie, Michel Stchakovsky, Sophie Neveu, Damien Jamon, Enric Garcia-Caurel

## ► To cite this version:

Yann Battie, Michel Stchakovsky, Sophie Neveu, Damien Jamon, Enric Garcia-Caurel. Synthesis and study of  $\gamma$ -Fe<sub>2</sub>O<sub>3</sub> and CoFe<sub>2</sub>O<sub>4</sub> based ferrofluids by means of spectroscopic Mueller matrix ellipsometry. *Journal of Vacuum Science & Technology B, Nanotechnology and Microelectronics*, 2019, 37 (6), pp.062929. 10.1116/1.5121286 . ujm-02396890

**HAL Id: ujm-02396890**

**<https://ujm.hal.science/ujm-02396890>**

Submitted on 28 Jan 2022

**HAL** is a multi-disciplinary open access archive for the deposit and dissemination of scientific research documents, whether they are published or not. The documents may come from teaching and research institutions in France or abroad, or from public or private research centers.

L'archive ouverte pluridisciplinaire **HAL**, est destinée au dépôt et à la diffusion de documents scientifiques de niveau recherche, publiés ou non, émanant des établissements d'enseignement et de recherche français ou étrangers, des laboratoires publics ou privés.

# Synthesis and Study of $\gamma$ -Fe<sub>2</sub>O<sub>3</sub> and CoFe<sub>2</sub>O<sub>4</sub> Based Ferrofluids by Means of Spectroscopic Mueller Matrix Ellipsometry

Yann Battie <sup>1</sup>, Michel Stchakovsky <sup>2,a)</sup>, Sophie Neveu <sup>3</sup>, Damien Jamon <sup>4</sup>, Enric Garcia-Caurel <sup>5</sup>

<sup>1</sup>LCP-A2MC, Institut Jean Barriol, Université de Lorraine, 1 Bd Arago, 57070 Metz, France

<sup>2</sup>HORIBA Scientific, 14 Boulevard Thomas Gobert, Passage Jobin Yvon, 91120 Palaiseau, France

<sup>3</sup>Laboratoire PHENIX, Sorbonne University, 4 Place Jussieu, 75252 Paris, France

<sup>4</sup>Laboratoire Hubert Curien, Université de Saint-Etienne, 42000 St Etienne, France

<sup>5</sup>LPICM, Ecole Polytechnique, 91120 Palaiseau, France

a) Electronic mail: [michel.stchakovsky@horiba.com](mailto:michel.stchakovsky@horiba.com)

Ferrofluids are colloidal suspensions generally composed of ferromagnetic or ferrimagnetic nanoparticles (NPs). In the present study, we have focused on the ellipsometric characterization of two types of ferrofluids: one constituted of maghemite ( $\gamma$ -Fe<sub>2</sub>O<sub>3</sub>) NPs and one of Cobalt ferrite (CoFe<sub>2</sub>O<sub>4</sub>) NPs. The optical properties of the NPs are extracted from the ellipsometric spectra by using the Maxwell-Garnett effective medium approximations. As expected, Mueller Matrix (MM) measurements reveal that the ferrofluid becomes anisotropic under influence of a magnetic field. We correlate this anisotropy to the preferential orientation of NPs along the magnetic field.

## I. INTRODUCTION

Spectroscopic Ellipsometry (SE) is an optical characterization technique that is popular in plenty of domains of solid-state physics. Generally, SE is applied to characterize thin film structures at the air-solid interface and sometimes applied to study phenomena at liquid-solid interfaces. In our previous work [1], we presented several results illustrating the feasibility of liquid characterization by SE. This work is the extension of these first results applied to ferrofluids that are non-standard liquids due to their magneto-induced anisotropic optical properties [2] investigated here with MM approach.

Ferrofluids are colloidal suspension composed of ferromagnetic or ferrimagnetic NPs with size generally ranging from 5 to 25 nm. At macroscopic scale, these suspensions have superparamagnetic properties. Stabilized ferrofluids have been synthesized for the first time about 50 years ago [3] and have present and future application in several domains such as mechanics as lubricant or seals [4], in optics such as tunable components [5] or in medicine for potential heat source in magnetic hyperthermia [6]. In this work 2 types of ferrofluids have been studied:  $\text{CoFe}_2\text{O}_4$  and  $\gamma\text{-Fe}_2\text{O}_3$  water suspensions. We will refer to them in the following sections as Cobalt ferrite and maghemite respectively. Optical and magneto-optical (MO) properties of these materials have been studied extensively as thin films [7,8], or as NPs embedded in dielectric matrix [9, 10]. Other MO studies on these materials in ferrofluid phase also exist [11] but were often restricted to single wavelength analysis. Our work consists of a MO study on Cobalt ferrite and maghemite ferrofluids over the visible near infrared spectral range.

In the last 15 years, MM studies have generated an increasing interest among the community of ellipsometry users. New insight have appeared related to instrumentation [12, 13], related to applications for nano-structured and anisotropic materials [14, 15], together with developments related to the corresponding theories [16-18]. In this paper, we perform a qualitative approach using a modified commercial MM instrument to monitor the dynamic anisotropic response of NP ferrofluid solutions under magnetic field influence. It confirms that the MM is a suitable tool to investigate the dynamic collective orientation of NPs.

## II. SYNTHESIS AND NON POLARIMETRIC CHARACTERIZATIONS

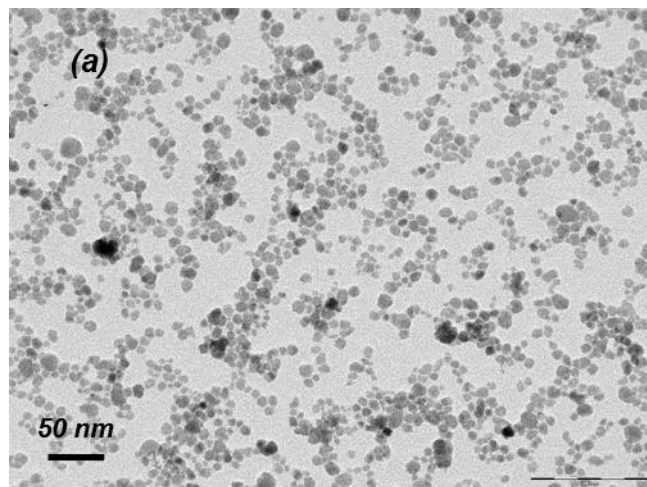
Magnetic nanoparticles (maghemite and cobalt ferrite) are obtained using a coprecipitation process developed in PHENIX lab a long time ago [19]. In a typical experimental procedure, corresponding to the cobalt ferrite,  $\text{CoCl}_2 \cdot 6\text{H}_2\text{O}$  ( $m = 3.026 \text{ g}$ ) was dissolved in an acidic solution ( $\text{HCl}$ ,  $0.02 \text{ mol/L}$ ,  $v = 250 \text{ mL}$ ).  $\text{FeCl}_3$  solution ( $[\text{Fe(III)}] = 2.12 \text{ mol/L}$ ,  $v = 12 \text{ mL}$ ) was added and the mixture was heated to boiling. Boiling aqueous solution of  $\text{NaOH}$  ( $c = 10 \text{ mol/L}$ ,  $v = 20 \text{ mL}$ ) was quickly added to the ionic metallic solution under stirring. A black precipitate immediately formed. Stirring and boiling were maintained during 1 hour. After cooling to room temperature, the precipitate was isolated and washed once with water. A nitric acid treatment was performed ( $[\text{HNO}_3] = 2 \text{ mol/L}$ ,  $v = 100 \text{ mL}$ ) in order to eliminate hydroxide species eventually present after the heating treatment. This allows also to obtain cationic nanoparticles. In order to stabilize the

This is the author's peer reviewed, accepted manuscript. However, the online version of record will be different from this version once it has been copyedited and typeset.  
PLEASE CITE THIS ARTICLE AS DOI: 10.1116/1.5121286

nanoparticles in acidic medium, a ferric nitrate treatment is performed:  $\text{Fe}(\text{NO}_3)_3$  solution was added and the mixture was heated to boiling half an hour. Magnetic NPs thus obtained were washed three times with acetone and two times with ether before to be dispersed in 10 mL of distilled water. We obtained by this process an aqueous magnetic fluid at pH = 2. To synthesize maghemite particles,  $\text{CoCl}_2$  is replaced by  $\text{FeCl}_2$ .

The concentrations of the metallic species were determined by atomic absorption spectrometry measurements using a Perkin-Elmer Analyst 100 apparatus, after dissolution of the NPs in concentrated hydrochloric acid. Taking into account the molar volume of magnetic oxides, the NPs volume fractions in ferrofluids are finally determined by multiplying the molar concentration of iron by a proper coefficient, (1.631 for maghemite and 2 for Cobalt ferrite) [19].

Transmission electron microscopy (Jeol 100 CX2) images of both ferrofluids are depicted in Fig. 1 for maghemite (a) and cobalt ferrite (b). The NPs have irregular spheroidal shape and their average diameters are in the range of 12 nm and 25 nm for maghemite and cobalt ferrite respectively.



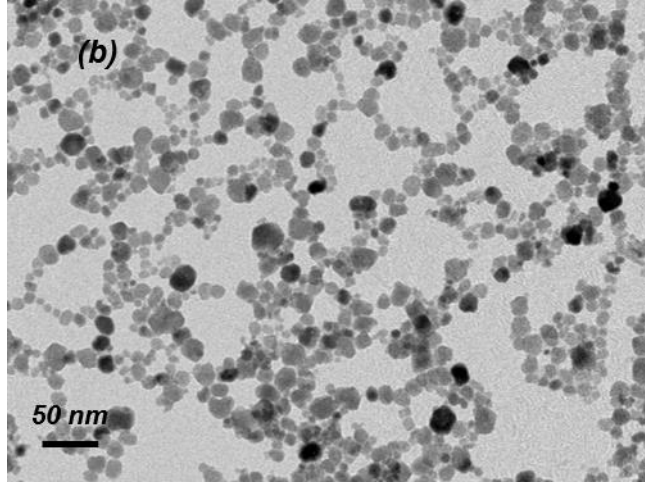


Fig. 1. TEM images of maghemite (a), and cobalt (b) NPs.

NP sizes have also been investigated by Dynamic Light Scattering technique (DLS) using a HORIBA SZ-100 instrument. Its results presented on Fig. 2 are perfectly correlated with results obtained by microscopy. One measures highest density of NP with diameters 12 nm and 25 nm for maghemite and cobalt respectively. 90% of NP have diameters within the intervals [10 nm , 20 nm] or [20 nm , 40 nm] for maghemite and cobalt respectively.

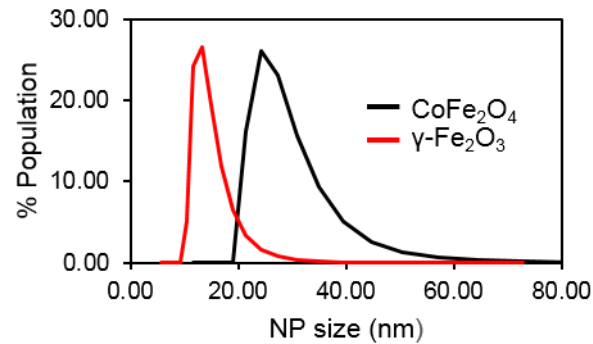


Fig. 2. DLS measurements expressed as NP population density as a function of size.

### III. POLARIMETRIC CHARACTERIZATIONS

#### A. Spectroscopic ellipsometry studies

UVISEL+ phase modulated spectroscopic ellipsometer by HORIBA Scientific has been used to evaluate transmission spectra of ferrofluids and to characterize their optical indices. This phase modulation ellipsometer, measures two parameters  $I_s$  and  $I_c$ , which are related to ellipsometric angles and MM elements for isotropic systems by the following equations:

$$I_s = \sin 2\psi \sin \Delta = m_{34} \text{ and } I_c = \sin 2\psi \cos \Delta = m_{33} \quad (1)$$

The water based ferrofluids, investigated by transmission spectroscopy have a NPs volume fraction of 0.2%. The air referenced transmission measurements, illustrated on Fig. 3, are performed through a 100  $\mu\text{m}$  thick fused silica cell. From these spectra, it has been decided to focus our polarimetric studies in the 500 – 1000 nm spectral range where both suspensions show enough transparency properties.

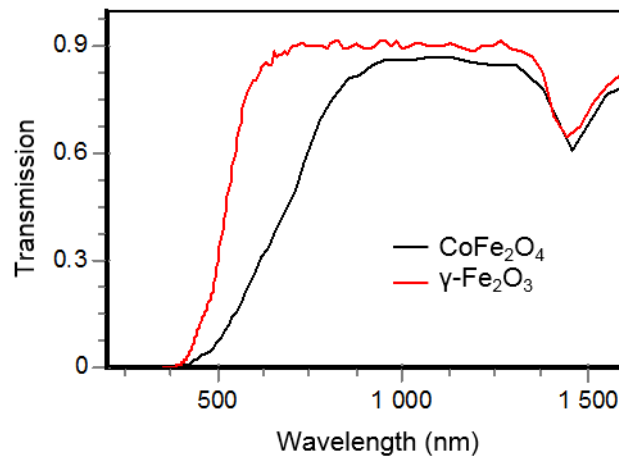


Fig. 3. Transmission spectra of ferrofluids solutions for 0.2% NPs volume fraction.

The ellipsometric response of the ferrofluid has been studied in a dedicated prism cell devoted to the characterization of liquids [1,20]. The NPs solution is introduced between a silicon wafer and a silica prism. The thickness of the liquid layer, controlled by a polymer spacer, is 125  $\mu\text{m}$ . The angle of incidence which depends on the angle of the prism, is set at  $55^\circ$ . This cell combines several advantages such as being insensitive to liquid surface waves, being sensitive to extinction coefficients as low as  $10^{-5}$  to  $10^{-6}$ , being usable only with 20  $\mu\text{l}$  of liquid but mostly, having the advantage to extract simultaneously real and imaginary part of refractive index, either isotropic or not.

In the modeling process, the goal was to extract optical properties of maghemite and cobalt NPs. To do so, 3 concentrations of the two ferrofluids have been analyzed by multimodeling approach. The models consist in a silicon wafer covered by a 125  $\mu\text{m}$  layer of ferrofluid with specific concentration. The ambient is the silica prism. The effective dielectric function of ferrofluid  $\epsilon_{eff}$  is calculated from the Maxwell-Garnett effective medium equation,

$$\frac{\epsilon_{eff} - \epsilon_m}{\epsilon_{eff} + \epsilon_m} = f \frac{\epsilon_{np} - \epsilon_m}{\epsilon_{np} + \epsilon_m} \quad (2)$$

where  $f$  is the volume fraction of NPs,  $\epsilon_m$  the dielectric function of water obtained in our previous work, and  $\epsilon_{np}$  the dielectric function of NPs. This latter is described by a combination of 2 Tauc-Lorentz dispersion formula for both ferrofluids [21].

In both multimodels, parameters of adjustments were only dispersion parameters of the NPs, their volume fraction being fixed according to experimental conditions of dilutions in the range of 0.002 % to 0.01 %. Fig. 4 compares the measured to the modeled ellipsometric spectra of ferrofluids. The model reproduces properly the ellipsometric measurement performed for the 3 concentrations of the ferrofluids.



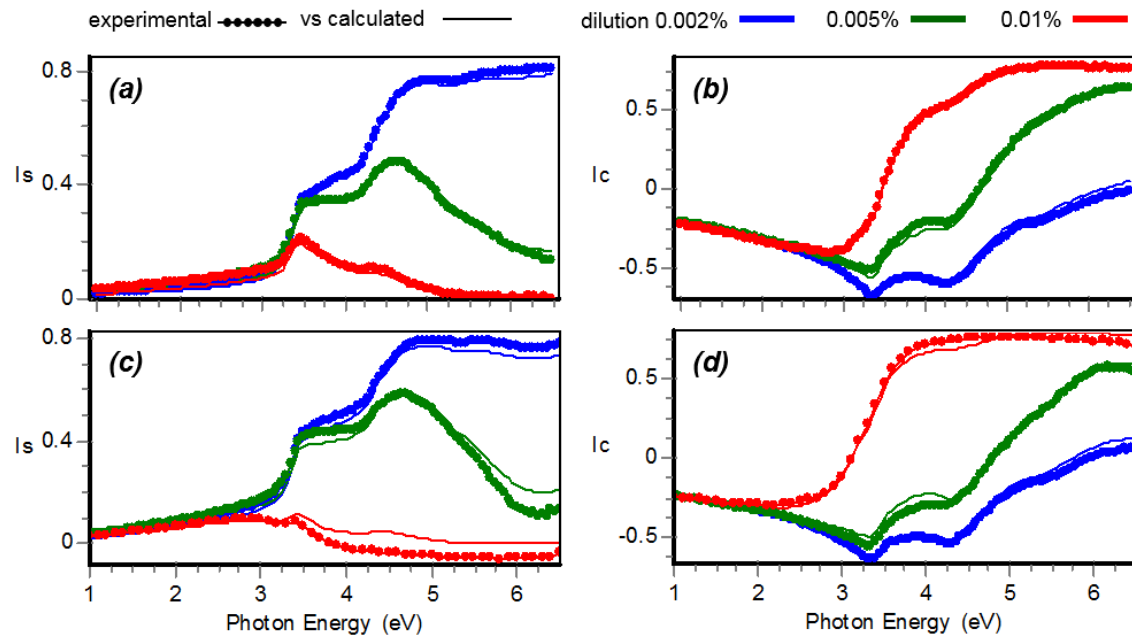


Fig. 4. Comparisons between experimental and calculated ellipsometric data  $I_s$  and  $I_c$ , after simultaneous fitting of optical properties of ferrofluids, for 3 concentrations of NPs. (a) and (b) is for the case of maghemite, whereas (c) and (d) is for the case of cobalt ferrite.

As a result of this effective medium study, we have obtained the optical indices of the 3 different concentrations of ferrofluids. The indices for concentrations of 0.01% are displayed on Fig. 5 (a) and (b) for maghemite and cobalt respectively. Fig. 5 (c) and (d) are the indices of the isolated nanoparticles of  $\gamma$ - $\text{Fe}_2\text{O}_3$  and  $\text{CoFe}_2\text{O}_4$  respectively. Due to the low volume fraction of NPs, the real part of the effective refractive index of suspension is close to the one of water. The presence of NPs is mainly observed in the imaginary part of the effective refractive index. As expected from transmission measurements, the cobalt ferrofluids exhibit a higher  $k$  onset value in the visible range than the maghemite ones. The refractive index of NPs differs from the tabulated one for bulk materials. This difference

can be due to confinement effect and to the lack of accurate data in the literature for these materials.

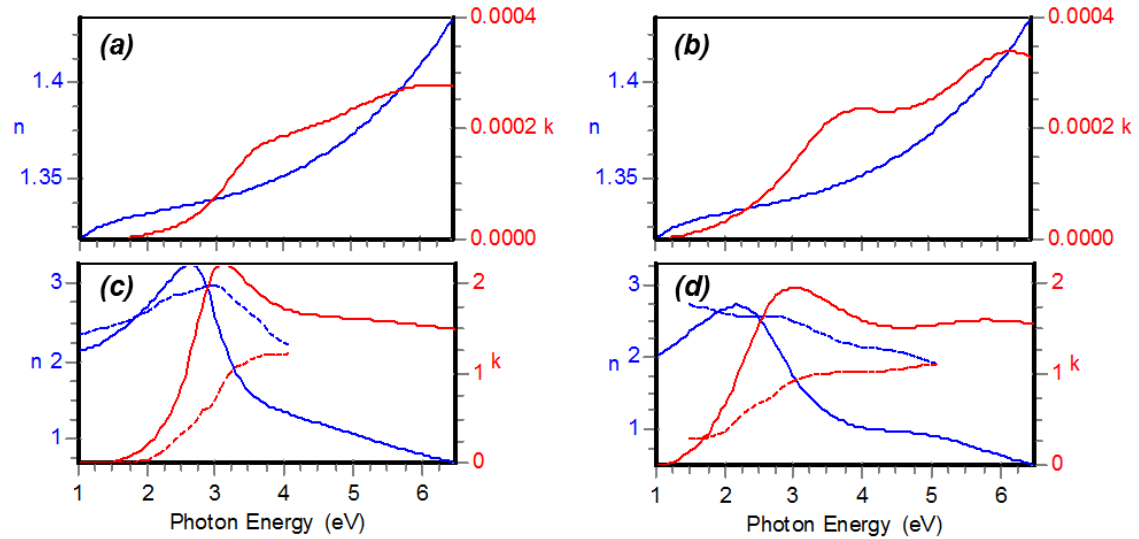


Fig. 5. Effective optical indices of maghemite (a), and cobalt (b) ferrofluids with 0.01% volume fraction of NPs. Optical indices of maghemite (c), and cobalt (d) NPs. Dashed lines are for bulk materials from the ref [22].

### ***B. Magneto-optic Mueller matrix studies***

The following step of the study completes a previous work [23] as it involves the complete MM characterization of ferrofluids in the prism cell, under the influence of magnetic field. The field was produced by a combination of two neodymium magnets. The magnets assembly was motorized and able to rotate around a vertical axis. This azimuth angle is covering an amplitude of  $360^\circ$ . Field lines are illustrated on Fig. 6 when they lay in the plane of incidence of the polarimeter setup: a smartSE from HORIBA illustrated on Fig. 7.

This is the author's peer reviewed, accepted manuscript. However, the online version of record will be different from this version once it has been copyedited and typeset.  
PLEASE CITE THIS ARTICLE AS DOI: 10.1116/1.5121286

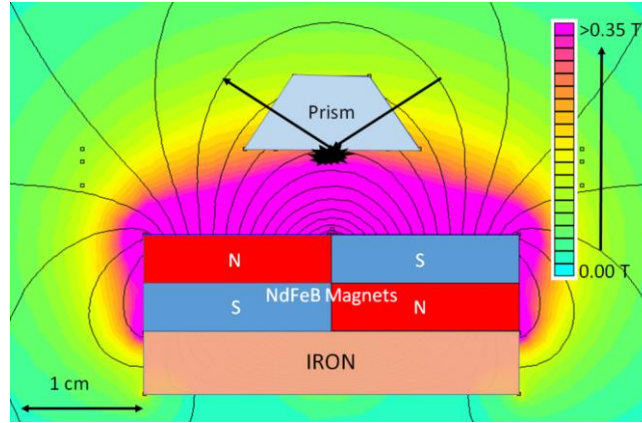


Fig. 6. Schematic of magnetic field lines in the plane of incidence, simulated with FEMM42 software [24]. The bold arrows illustrate the ellipsometric beam path. The probed volume of liquid is located under the silica prism. This volume is localized 1 cm above the magnet system, where the magnetic field is homogeneous in the range of 0.2 T.

This is the author's peer reviewed, accepted manuscript. However, the online version of record will be different from this version once it has been copyedited and typeset.  
PLEASE CITE THIS ARTICLE AS DOI: 10.1116/1.5121286

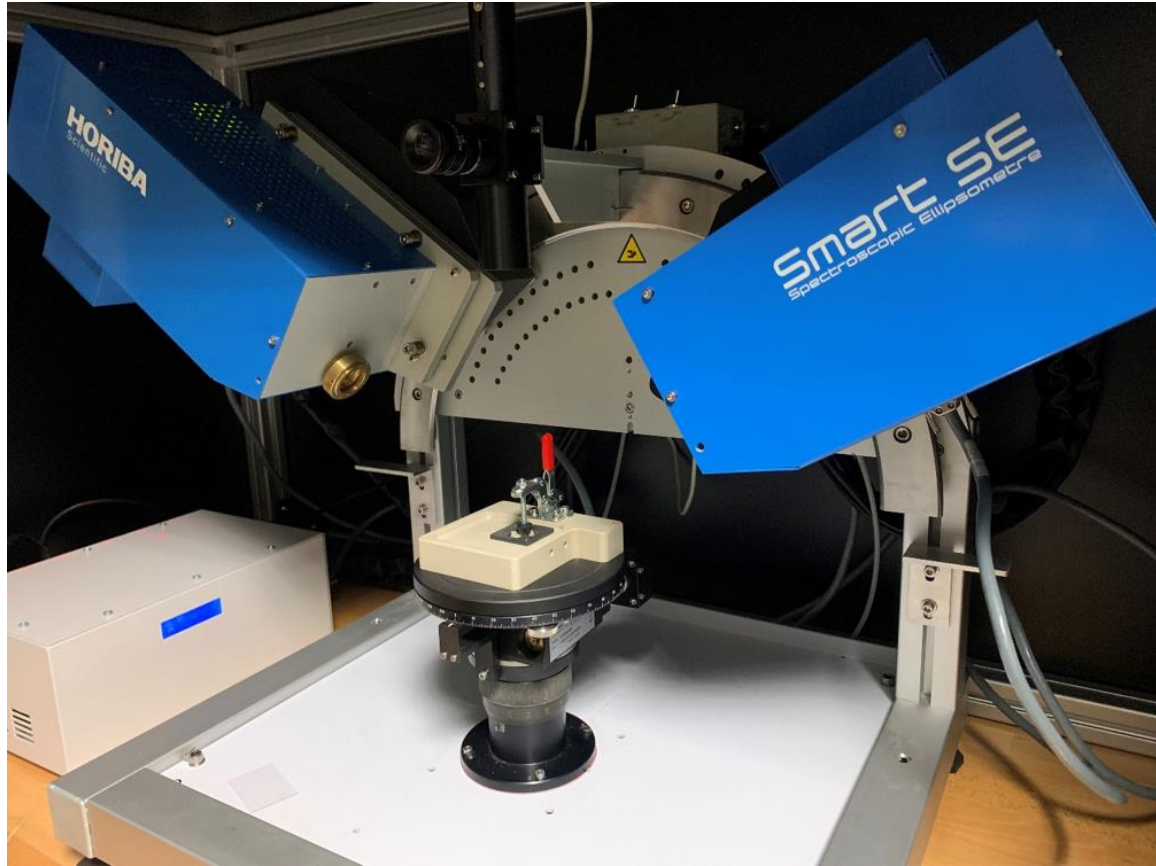


Fig. 7. Experimental setup for MO polarimetric experiments. The angle of incidence is  $55^\circ$ . The prism liquid cell and the sample holder including magnet are also shown.

For both ferrofluids, in absence of magnetic field, the off-diagonal elements  $m_{13}$ ,  $m_{14}$ ,  $m_{23}$ ,  $m_{24}$ ,  $m_{31}$ ,  $m_{32}$ ,  $m_{41}$  and  $m_{42}$  of MM were measured equal to 0, suggesting that the ferrofluids are initially isotropic. Normalized ( $m_{11} = 1$ ) MM recordings at selected wavelengths, for 0.2% concentrated ferrofluids, as a function of azimuth of magnetic field are illustrated in Fig. 8. The plateaus that can be observed on this figure are explained by several successive measurements taken at fixed azimuths. They illustrate the time response of the ferrofluids under excitation and their stability during measurements.

This is the author's peer reviewed, accepted manuscript. However, the online version of record will be different from this version once it has been copyedited and typeset.  
PLEASE CITE THIS ARTICLE AS DOI: 10.1116/1.5121286

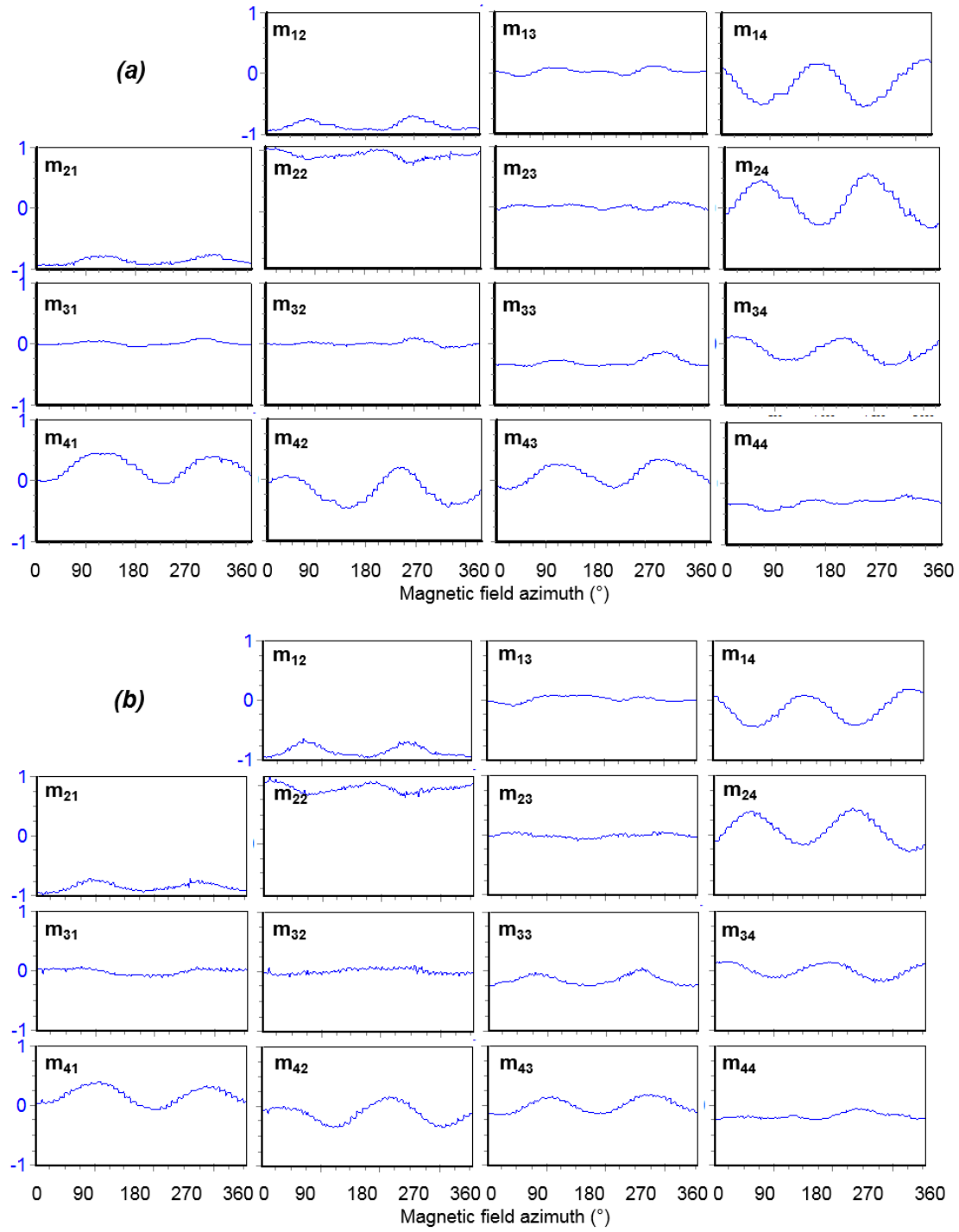


Fig. 8. MM measurements at selected wavelength for both ferrofluids as a function of azimuth of applied magnetic field. (a) is for maghemite at 574 nm and (b) is for Cobalt ferrite at 750 nm.

Qualitatively, both ferrofluids show similar responses, all elements of the MM showing significant fluctuations with magnetic field orientation. No significant depolarization of these MM have been observed. The off-diagonal elements of the MM strongly depend on the azimuth of the magnetic field that is the source of an optical anisotropy inside the ferrofluids. Both linear and circular birefringences (LB and CB) coexist in the systems under investigation. The CB originates from the Faraday effect that aligns the magnetic momentum of the nanoparticles along the magnetic field. As the Faraday effect is a non-reciprocal effect, its optical signature should have a period of  $360^\circ$  with azimuth. On the other hand, the LB originates from preferential orientation of non-spherical NPs along the magnetic field. Such effect induced by the NP orientation should have a period of  $180^\circ$ . It is what one mainly observes in Fig. 6, with a periodicity of  $180^\circ$  rather than  $360^\circ$ . We conclude that although NPs are nearly spherical, the deviation from spherical shape has a significant impact on MO measurements because their long axis lays along the magnetic field and thus, that the LB is the main source of anisotropy.

Birefringences analysis using MM decompositions techniques do not apply easily in our case because our experiments are of oblique incidence reflection type. At this stage, the modeling of these experiments is beyond the scope of this preliminary work and will be the object of a future publication.

#### IV. SUMMARY AND CONCLUSIONS



In this work, we have presented an optical and a MO characterization of maghemite and cobalt ferrite ferrofluids. In a first part we have characterized these ferrofluids' optical properties by spectroscopic ellipsometry. We also could extract through an inversion of effective medium approximation the complex indices of both  $\gamma$ -Fe<sub>2</sub>O<sub>3</sub> and CoFe<sub>2</sub>O<sub>4</sub> nanoparticles. In a second part we have investigated the MO response of the ferrofluids in a dedicated cell under a controlled magnetic excitation. At this stage we have shown the orientation of slightly anisotropic NPs under a magnetic field. Quantitative modeling to quantify LB and CB is planned for a near future campaign of analysis.

- <sup>1</sup>M. Stchakovsky, Y. Battie, and A. En-Naciri, *Appl. Surf. Sci.* **421**, 802–806 (2017)
- <sup>2</sup>Q. Majorana, *C. R. Acad. Sci. Paris* **135**, 159 (1902)
- <sup>3</sup>S. S. Papell, U.S. Patent N° 3215572 (1965)
- <sup>4</sup>M. Mizumoto, and H. Inoue, *J. Magn. Magn. Mater.* **65**, 2-3, 385-388 (1987)
- <sup>5</sup>J. Philip, T. Jaykumar, P. Kalyanasundaram, and B. Raj, *Meas. Sci. Technol.* **14**, 1289 (2003)
- <sup>6</sup>J. Carrey, B. Mehdaoui, and M. Respaud, *J. Appl. Phys.* **109**, 83921 (2011)
- <sup>7</sup>C. E. Barrera, J. C. Martinez-Flores, G. F. Gonzalez, M. Ortega-Lopez, and R. C. Rosas, *The Open Surface Science Journal* **5**, 9-16 (2013)
- <sup>8</sup>R. Illa, R. Jesko, R. Silber, O. Zivotsky, K. M. Kutlakova, L. Matejova, M. Kolencik, J. Pistora, and J. Hamrle, *Mater. Res. Bull.* **117**, 96-102 (2019)
- <sup>9</sup>M. Zamani, and A. Hocini, *Opt. Mater.* **58**, 306-309 (2016)
- <sup>10</sup>F. Bentivegna, M. Nyvlt, J. Ferré, J. P. Jamet, A. Brun, S. Visnovsky, and R. Urban, *J. Appl. Phys.* **85**, 2270-2278 (1999)
- <sup>11</sup>J. Fun, J. Li, Y. Lin, X. Liu, H. Miao, and L. Lin, *Sci. China Phys. Mech.* **55**, 1404-1411 (2012)
- <sup>12</sup>B. Laude-Boulesteix, A. De Martino, B. Drévilion, and L. Schwartz, *Appl. Opt.* **43**, 2824-2832 (2004)
- <sup>13</sup>S. Liu, X. Chen, and C. Zhang, *Thin Solid Films* **584**, 176 (2015)
- <sup>14</sup>N. Guth, S. Varault, J. Grand, G. Guida, N. Bonod, B. Gallas, and J. Rivory, *Thin Sol. Films*, **571**, 405-409 (2014)
- <sup>15</sup>C. De Dios, A. Jimenez, F. Garcia, A. Garcia-Martin, A. Cebollada, and G. Armelles, *Opt. Express* **27**, 21142-21152 (2019)
- <sup>16</sup>O. Arteaga, and B. Kahr, *J. Opt. Soc. Am. B* **36**, F72-F83 (2019)
- <sup>17</sup>O. Arteaga, and R. Ossikovski, *J. Opt. Soc. Am. A* **36**, 403-415 (2019)

<sup>18</sup>J. J. Gil-Perez, and R. Ossikovski, *Polarized Light And The Mueller Matrix Approach* (CRC Press, Taylor and Francis Group, 2016)

<sup>19</sup>S. Lefebure, E. Dubois, V. Cabuil, S. Neveu, and R. Massart, *J. Mater. Res.* **13**, 2975 (1998)

<sup>20</sup>A. Resano-Garcia, Y. Battie, A. En-Naciri, S. Akil, and N. Chaoui, *J. Chem. Phys.* **142**, 134108 (2015)

<sup>21</sup>J. Jellison, and M. Modine, *Appl. Phys. Lett.* **69**, 371-373, (1996)

<sup>22</sup>J. W. D. Martens, W. L. Peeters, and M. Erman, *Solid State Commun.* **41**, 9, 667-669 (1982)

<sup>23</sup>D. Jamon, *J. Magn. Magn. Mater.* **321**, 1148-1154 (2009)

<sup>24</sup>D. C. Meeker, *Finite Element Method Magnetics*, Version 4.2, 28 Feb 2018 Build, <http://www.femm.info>

Fig. 1. TEM images of maghemite (a), and cobalt (b) NPs.

Fig. 2. DLS measurements expressed as NP population density as a function of size.

Fig. 3. Transmission spectra of ferrofluids solutions for 0.2% NPs volume fraction.

Fig. 4. Comparisons between experimental and calculated ellipsometric data  $I_s$  and  $I_c$ , after simultaneous fitting of optical properties of ferrofluids, for 3 concentrations of NPs. (a) and (b) is for the case of maghemite, whereas (c) and (d) is for the case of cobalt ferrite.

Fig. 5. Effective optical indices of maghemite (a), and cobalt (b) ferrofluids with 0.01% volume fraction of NPs. Optical indices of maghemite (c), and cobalt (d) NPs. Dashed lines are for bulk materials from the ref [22].

Fig. 6. Schematic of magnetic field lines in the plane of incidence, simulated with FEMM42 software [24]. The bold arrows illustrate the ellipsometric beam path. The probed volume of liquid is located under the silica prism. This volume is localized 1 cm above the magnet system, where the magnetic field is homogeneous in the range of 0.2 T.

Fig. 7. Experimental setup for MO polarimetric experiments. The angle of incidence is  $55^\circ$ . The prism liquid cell and the sample holder including magnet are also shown.

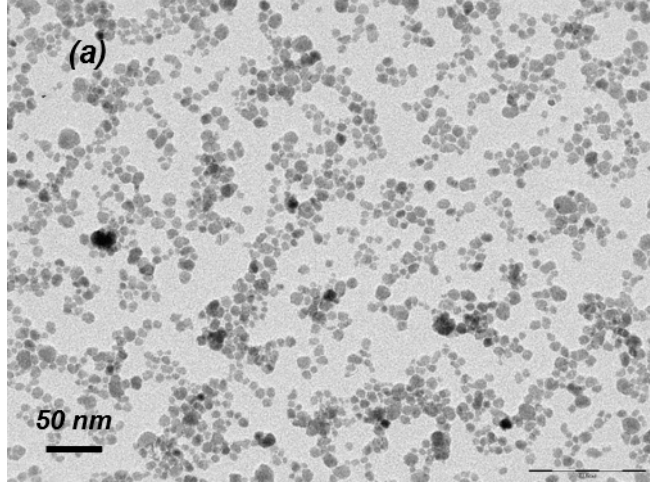


This is the author's peer reviewed, accepted manuscript. However, the online version of record will be different from this version once it has been copyedited and typeset.

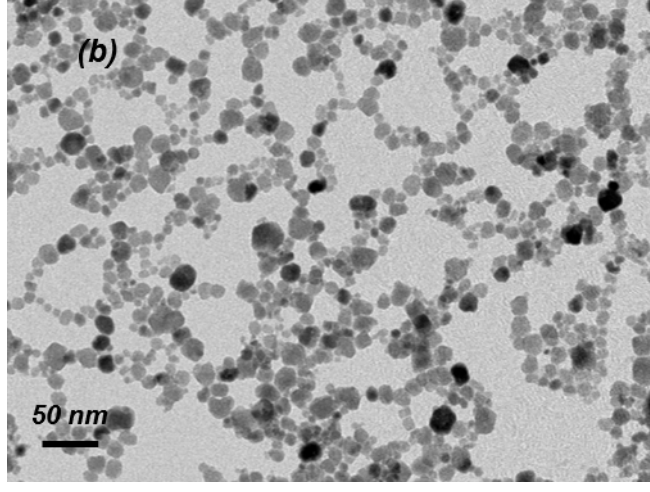
PLEASE CITE THIS ARTICLE AS DOI: 10.1116/1.5121286

Fig. 8. MM measurements at selected wavelength for both ferrofluids as a function of azimuth of applied magnetic field. (a) is for maghemite at 574 nm and (b) is for Cobalt ferrite at 750 nm.

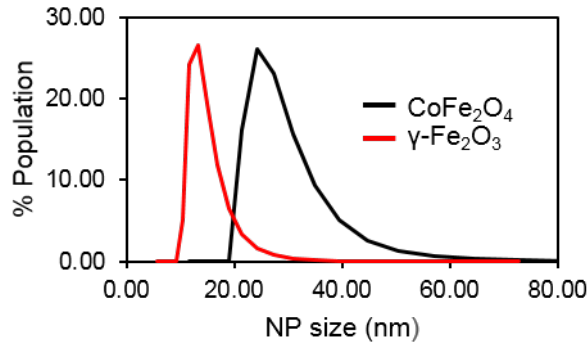
This is the author's peer reviewed, accepted manuscript. However, the online version of record will be different from this version once it has been copyedited and typeset.  
**PLEASE CITE THIS ARTICLE AS DOI: 10.1116/1.5121286**



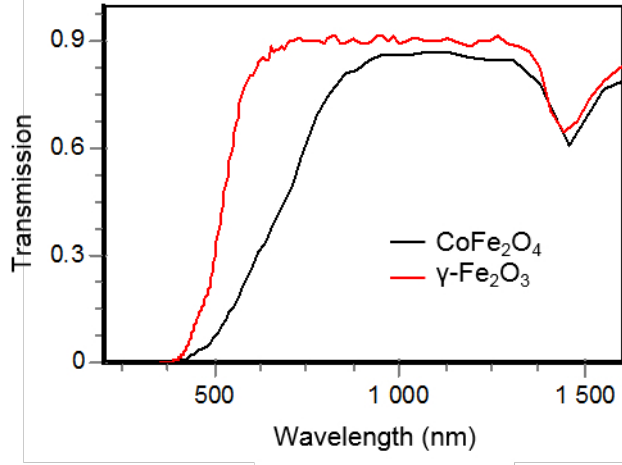
This is the author's peer reviewed, accepted manuscript. However, the online version of record will be different from this version once it has been copyedited and typeset.  
PLEASE CITE THIS ARTICLE AS DOI: 10.1116/1.5121286



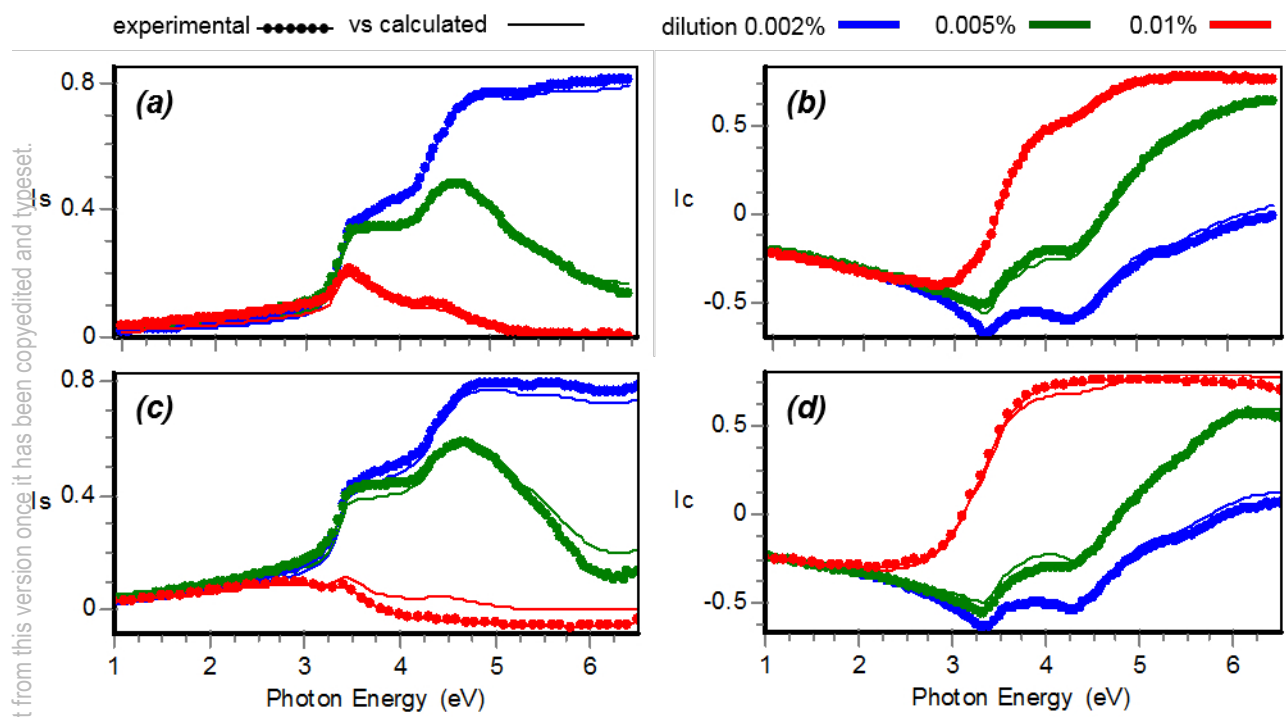
This is the author's peer reviewed, accepted manuscript. However, the online version of record will be different from this version once it has been copyedited and typeset.  
PLEASE CITE THIS ARTICLE AS DOI: 10.1116/1.5121286



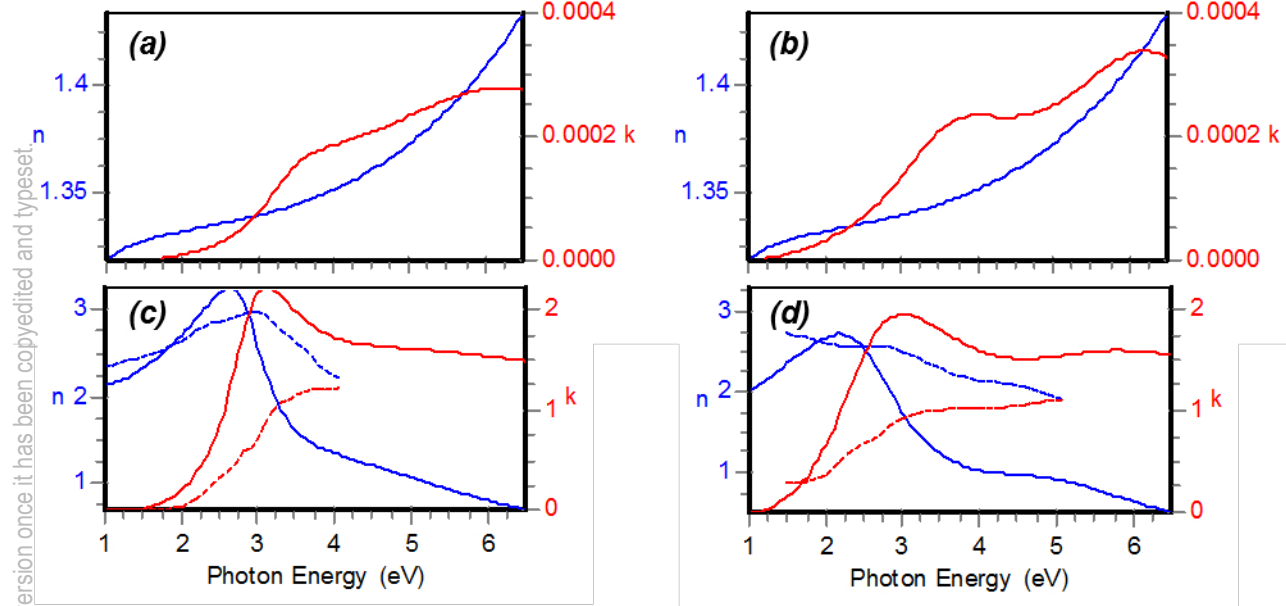
This is the author's peer reviewed, accepted manuscript. However, the online version of record will be different from this version once it has been copyedited and typeset.  
PLEASE CITE THIS ARTICLE AS DOI: 10.1116/1.5121286



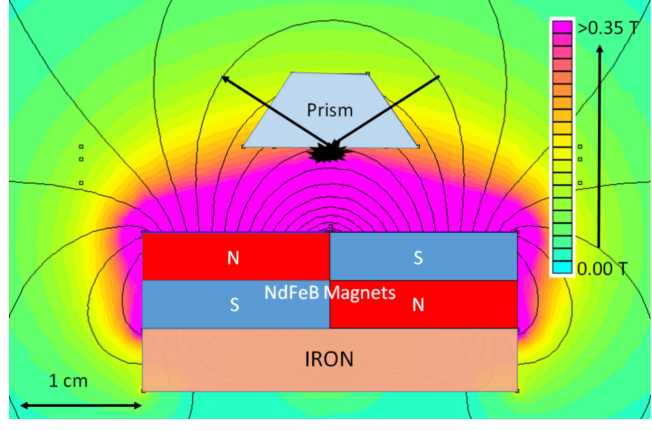
This is the author's peer reviewed, accepted manuscript. However, the online version of record will be different from this version once it has been copyedited and typeset.  
PLEASE CITE THIS ARTICLE AS DOI: 10.1116/1.5121286



This is the author's peer reviewed, accepted manuscript. However, the online version of record will be different from this version once it has been copyedited and typeset.  
PLEASE CITE THIS ARTICLE AS DOI: 10.1116/1.5121286

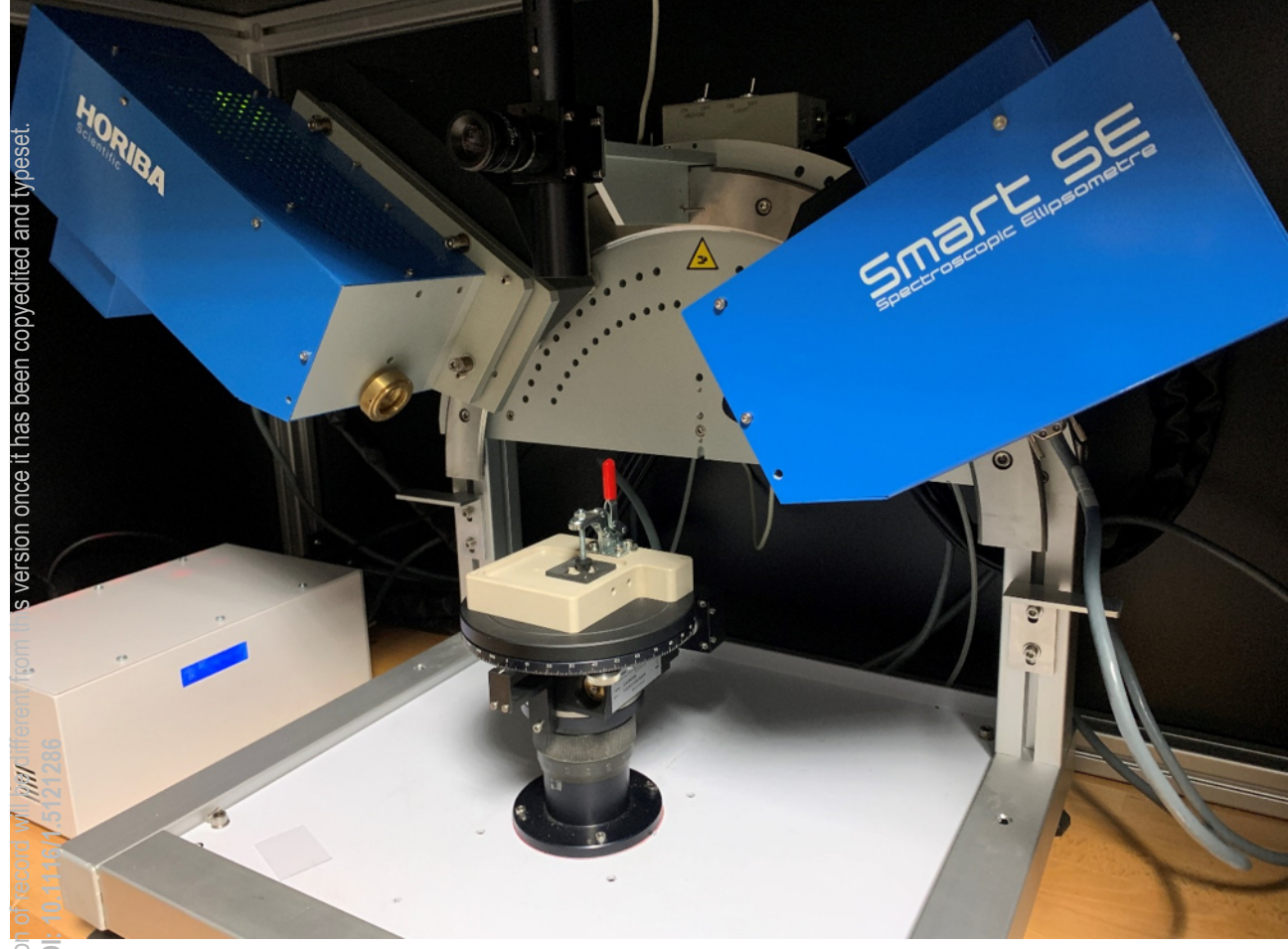


This is the author's peer reviewed, accepted manuscript. However, the online version of record will be different from this version once it has been copyedited and typeset.  
PLEASE CITE THIS ARTICLE AS DOI: 10.1116/1.5121286





This is the author's peer reviewed, accepted manuscript. However, the online version of this article will differ from this version once it has been copyedited and typeset.  
PLEASE CITE THIS ARTICLE AS DOI: 10.1111/j.5421286



This is the author's peer reviewed, accepted manuscript. However, the online version of record will be different from this version once it has been copyedited and typeset.  
PLEASE CITE THIS ARTICLE AS DOI: 10.1116/1.5121286

